Songklanakarin J. Sci. Technol.
45 (5), 543–551, Sep. – Oct. 2023

http://www.sjst.psu.ac.th

Original Article

Optimal control of cuk converter using LQR

Deepak Kumar Singh*, Saibal Manna, and Ashok Kumar Akella

Department of Electrical Engineering,
National Institute of Technology Jamshedpur, Jharkhand, 831014 India

Received: 7 July 2021; Revised: 23 March 2023; Accepted: 27 July 2023

Abstract

In this paper, linear quadratic regulator (LQR) control is applied to a Cuk converter, and mathematical modeling of the converter is done using state space averaging (SSA) in continuous conduction mode (CCM). The primary focus is to design a controller for the converter and maintain output voltage within 1% of the prescribed value when there is a unit step disturbance in the input. The design done by using MATLAB improved control of the converter from that with a conventional controller when tested with disturbances. The controller did not influence the system's stability, when assessed from the Bode plot. Despite the existence of disturbances, the findings prove the efficacy of the suggested approach, and the proposed controller can track the desired output voltage in less than 14 ms. The LQR control was developed for various applications of the Cuk converter, such as in a photovoltaic system and a wind system.

Keywords: cuk converter, pole placement, integrator, bode plot, LQR

1. Introduction

DC-DC converters are commonly employed due to their great performance, to control the DC output voltage despite variations in the input voltage supply and load current. The literature presents different types of switched mode power converters, such as boost, buck, buck-boost and Cuk converter. The Cuk converter has the following features**:** continuous input and output current and a current-voltage-current converter (Cuk & Middlebrook, 1983). The Cuk converter has also decreased ripple currents, minimized switching losses, easy implementation, and it needs less components and basic drive circuitry than the other converters. Ideally, it offers great frequency response characteristics, allowing a highly stable feedback control to be realized. The benefit of the Cuk converter is that the output and input inductors produce a smooth current on both sides of the converter. At the same time, the buck, boost, and buck-boost have at least one side with pulsed current, even the single-ended primary inductor (SEPIC) (Selwan *et al*., 2015).

*Corresponding author
Email address: dksingh1946@gmail.com

The Cuk converter incorporates the features of boost and buck converters, which means that the output voltage can be either increased or decreased relative to the input voltage. The energy transfer between input and output is done using an inductor, and the operation is based on inductor voltage balance. The Cuk converter utilizes capacitive energy transfer, and the analysis can be subjected to the capacitor's current balance. As its primary energy-storage component, it uses a capacitor, which improves its efficiency. Since it provides ripple-free output, it can be employed in various applications such as renewable energy (Manna, Singh, & Akella, 2023), electric vehicles, and brushless DC motor drives (Thangavelusamy & Thirumeni, 2019).

The small signal analysis and modeling of converters in CCM are employed to change the output voltage of the converter with several traditional methods, such as Z-N tuned proportional integral (PI), linear control, or averaging circuit method, and the output of the converter can be controlled. However, the outcome achieved is unsatisfactory under different operating points, with parameter sensitivity variation, and instability due to changes in line and load (Kathi, Ayachit, Saini, Chadha, & Kazimierczuk, 2018; Pierkiewicz & Tollik, 1988; Sira-Ramirez & Silva-ortigoza, 2006).

To overcome these disadvantages, robust non-linear methods such as current control, voltage control and LQR have

been employed to improve the Cuk converter's output. Due to its versatility and robustness to disruptions, LQR has gained importance among these control techniques. The classic LQR strategy begins with the cost optimization or performance index function. Thus, in order to seek desired output, the designer should weigh which states are more relevant in the control operation. Several researchers have initiated this feature of LQR control to apply this method successfully in power electronics (Umamaheswari & Uma, 2013).

Cuk converters are commonly employed in applications such as wind energy systems (Su, Gong, Pan, Gao, & Wang 2010), photovoltaic systems (Chung, Tse, Hui, Mok, & Ho 2003), electric vehicles (Fan, Ge, & Hua, 2010; Jose & Mohan, 2003), radar transmitting and receiving systems (McGee & Nelms, 2004), light-emitting diode drivers (De Britto *et al*., 2008), telecommunications systems (Aboulnaga & Emadi, 2004), exercise bicycle energy storage systems (Janjornmanit, Yachiangkam, & Kaewsingha, 2007), and compressor and motor control systems (Himmelstoss & Walter, 2010; Singh & Singh, 2010).

With great effort, the modeling, dynamics, controls, and stability of the Cuk converter are being examined. Cuk converter performances are recorded and regulated for sustainable slow-scale oscillation, chaos phenomena, and bifurcation (Amini & Nazarzadeh, 2008; Tse, Lai, & Iu, 2000; Wong, Wu, & Tse, 2008). The passivity-based control (Flores, Avalos, & Espinoza, 2011), state-space averaging and neural network (Mahdavi, Nasiri, Agah, & Emadi, 2005), model predictive control (Neely, Decarlo, & Pekarek, 2010), scaling factor and fuzzy logic (Balestrino, Landi, & Sani, 2002), nonlinear carrier control (Zane & Maksimovic, 1998), H-infinity control (Kugi & Schlacher, 1999), genetic algorithm (Poudeh, Eshtehardiha, & Ershadi, 2008), direct control method (Safari & Makhilef, 2011), sliding mode control and robust nonlinear control of radial basis functions (Medagam & Pourboghrat, 2006) are among control approaches applied to the Cuk converter. Performance measures such as robustness, fast response, chaos behavior enhancement, stability, and a wide range of operating points are found with these controllers.

A series of papers discussed recommendations for control of the Cuk converter. Table 1 briefly explains the methodology adopted for the Cuk converter in various applications.

As per the literature review, LQR-based output voltage control of the Cuk converter under unit step disturbance is not discussed yet. This paper proposes controller design for a Cuk converter using the LQR approach. The output voltage of the Cuk converter should change less than 1% during disturbances. Moreover, for control of output voltage of Cuk converter, the proposed LQR is compared to well-known techniques such as Full State Feedback Controller (FSFB), Full State Feedback with an Integrator (FSFBI), and Reduced Order State Estimators (ROSE) using MATLAB calculations, in time and frequency domain parameters.

This article is arranged as follows. Section 2 discusses switching stages and an SSA model of Cuk converter with its design computation. Section 3 describes the open-loop performance of the Cuk converter. In section 4, the control schemes for regulating converter output are presented. MATLAB results of the Cuk converter with the proposed controller are explained in Section 5, and Section 6 incorporates the conclusion.

Table 1. Summary of the various methods adopted in control of the Cuk converter

Author	Methodology	Remarks
Umamaheswari & Uma, 2013	Reduced order linear quadratic regulator (ROLQR) control	The ROLQR control is designed and analyzed in 3-ϕ system for power factor correction. The modification of performance characteristics of Cuk rectifier with load disturbance demonstrates the efficacy of ROLQR control. The suggested system provides controlled output voltage for step load fluctuations and power factor close to unity.
Lekić, Stipanović, & Petrović, 2018	Hysteresis switching - polytopic Lyapunov function (HS-PLF)	It implements a control scheme for the Cuk converter utilizing an HS-PLF. In contrast to earlier quadratic Lyapunov functions, it offers accurate computation of the ripple values of the state variables.
Xu, Zhao, & Fan, 2004	PWM - Phase shift control (PPS)	PPS is devised to reduce current stress, decrease conduction and switching losses. With a wider range of loads, the converter controlled by PPS can achieve zero-voltage-switching.
Chen, 2012	PI- Sliding mode control (PI-SMC)	A fourth-order Cuk converter is controlled by PI-SMC in a CCM. The suggested controller allows the Cuk converter to operate over a wide range of operating points having maximum switching frequency of not more than 100 KHz and a load voltage following accuracy of ±0.05V.
Selwan, Park & Gajic, 2015	Jump parameter linear optimal control (JP-LOC)	This work subjected the Cuk converter to a JP-LOC approach employed in photovoltaic systems. The optimum controller for the jump linear system with integral action is implemented and compared to the averaged Cuk converter model. In the case of the JP-LOC technique, the output depicts small ripples, while for the averaged Cuk model, the output shows 1.5 and 3 ripples.
Rayeen, Bose, & Dwivedi, 2018	Loop shaping method	As the Cuk converter is a non-minimal phase system by nature, designing a controller for it is a difficult task. The Graphical Loop Shaping approach for the Cuk converter is designed. The enhanced phase and gain margins are 80.5 degrees and 173dB, respectively.
Yousefi, Emami, Eshtehardiha, & Poudeh, 2008	Pole placement-Particle swarm optimization (PSO)	A pole placement controller, which is a linear controller, has the ability to regulate the Cuk converter's dynamic behaviour. The design of this controller can result in the best possible dynamic response by using Particle Swarm Optimization to determine the optimum coefficients of gains.
Poudeh, Eshtehardiha, & Ershadi, 2008	PID-Genetic algorithm (PID-GA)	DC-DC converters are non-linear and complicated to regulate due to their switching characteristics. The average technique can represent the system as a linear model, allowing linear control methods. The best dynamic response is achieved by using a genetic algorithm to calculate the PID's optimum coefficients during the development of PID controller.

2. Cuk Converter

Cuk converter consists of cascaded buck and boost converters with an intervening capacitor linked in series. It is a switching boost/buck-based step-down/step-up converter. In essence, the converter is made up of two parts**:** an input part and an output part. Unlike traditional DC-DC converters, which employ an inductor as a storage element, the capacitor is the principal storage element that transports energy from the input to the output part.

Figure 1 depicts the Cuk converter circuit diagram, which has a DC supply (V_{IN}), two inductors (L_{01} and L_{02}), two capacitors (C_{01} and C_{02}), a diode (D_1), and a switch (Q); and a resistive load (R_{03}) is applied.

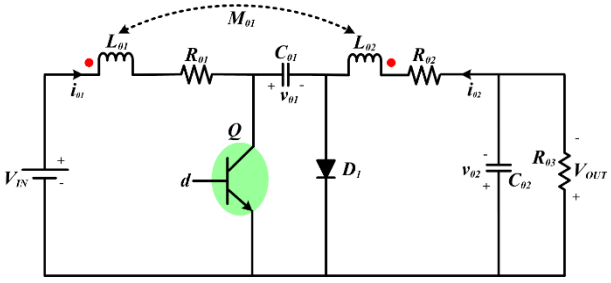

Figure 1. Cuk converter

2.1 Switching stages

There are two switching modes of the Cuk converter in CCM depending upon the switch (Q) condition, i.e., ON and OFF mode. When Q is in ON mode, the current (i_{01}) flows from the DC source through the inductor (L_{01}) and builds the inductor's magnetic field. The diode (D_1) is reverse-biased in this mode, and energy is dissipated in the output.

When Q is in OFF mode, current through the inductor cannot change instantaneously. The voltage across the inductor changes its polarity to maintain the current flow, D_1 is forward biased and capacitor C_{01} is charged, which contributes energy to the output. The sum of the currents i_{01} and i_{02} must be zero in steady state, and the charge conservation relation holds:

$$i_{01}t_{on} + i_{02}t_{off} = 0 \tag{1}$$

The relationship between the duty cycle (D_u), input voltage (V_{IN}) and output voltage (V_{OUT}) is given in equation (2). By changing D_u, an output voltage higher or lower than the input voltage can be obtained, and disturbances can also be eliminated during operation.

$$\frac{V_{OUT}}{V_{IN}} = \frac{D_u}{1-D_u} \tag{2}$$

2.2 SSA model

Modelling of the converter is more challenging than of other electrical circuits, since the circuit's nature depends on the switch position. The SSA technique is used to solve this problem. To avoid a non-minimum phase converter configuration, the Cuk converter is built with sufficient mutual inductance. This is a well-known technique employed to model switching converters. For the non-linear switching system, SSA offers a linear small-signal model. Here, the state vector considered is

$$x = [v_{02} \quad v_{01} \quad i_{02} \quad i_{01}]' \tag{3}$$

The inductor voltages ($v_{L_{01}}$ and $v_{L_{02}}$) are:

$$v_{L_{01}} = L_{01}\frac{di_{01}}{dt} + M_{01}\frac{di_{02}}{dt} \tag{4}$$

$$v_{L_{02}} = M_{01}\frac{di_{01}}{dt} + L_{02}\frac{di_{02}}{dt} \tag{5}$$

On re-arranging the above equations, we get

$$\frac{di_{01}}{dt} = \frac{L_{02}}{L_{01}L_{02}-{M_{01}}^2}v_{L_{01}} + \frac{-M_{01}}{L_{01}L_{02}-{M_{01}}^2}v_{L_{02}} \tag{6}$$

$$\frac{di_{02}}{dt} = \frac{-M_{01}}{L_{01}L_{02}-{M_{01}}^2}v_{L_{01}} + \frac{L_{01}}{L_{01}L_{02}-{M_{01}}^2}v_{L_{02}} \tag{7}$$

When Q is in ON mode:

$$v_{L_{01}} = V_{IN} - i_{01}R_{01} \tag{8}$$

$$v_{L_{02}} = v_{01} - v_{02} - i_{02}R_{02} \tag{9}$$

Substituting (8) and (9) into (6) and (7), we get

$$\frac{di_{01}}{dt} = \frac{M_{01}}{\kappa^2}v_{02} + \frac{-M_{01}}{\kappa^2}v_{01} + \frac{M_{01}R_{02}}{\kappa^2}i_{02} + \frac{-L_{02}R_{01}}{\kappa^2}i_{01} + \frac{L_{02}}{\kappa^2}V_{IN} \tag{10}$$

$$\frac{di_{02}}{dt} = \frac{-L_{01}}{\kappa^2}v_{02} + \frac{L_{01}}{\kappa^2}v_{01} + \frac{-L_{01}R_{02}}{\kappa^2}i_{02} + \frac{M_{01}R_{01}}{\kappa^2}i_{01} + \frac{-M_{01}}{\kappa^2}V_{IN} \tag{11}$$

where $\kappa^2 = L_{01}L_{02} - {M_{01}}^2$

When Q is in OFF mode:

$$v_{L_{01}} = V_{IN} - i_{01}R_{01} - v_{01} \tag{12}$$

$$v_{L_{02}} = -v_{02} - i_{02}R_{02} \tag{13}$$

Substituting (12) and (13) into (6) and (7), yields

$$\frac{di_{01}}{dt} = \frac{M_{01}}{\kappa^2} v_{02} + \frac{-L_{02}}{\kappa^2} v_{01} + \frac{M_{01}R_{02}}{\kappa^2} i_{02} + \frac{-L_{02}R_{01}}{\kappa^2} i_{01} + \frac{L_{02}}{\kappa^2} V_{IN} \quad (14)$$

$$\frac{di_{02}}{dt} = \frac{-L_{01}}{\kappa^2} v_{02} + \frac{M_{01}}{\kappa^2} v_{01} + \frac{-L_{01}R_{02}}{\kappa^2} i_{02} + \frac{M_{01}R_{01}}{\kappa^2} i_{01} + \frac{-M_{01}}{\kappa^2} V_{IN} \quad (15)$$

When Q is in ON mode, the state-space matrices are given by

$$\dot{x} = A_1 x + B_1 u \quad (16)$$

$$y = C_1 x + D_1 u \quad (17)$$

$$A_1 = \begin{bmatrix} \frac{-1}{R_{03}C_{02}} & 0 & \frac{1}{C_{02}} & 0 \\ 0 & 0 & \frac{-1}{C_{01}} & 0 \\ \frac{-L_{01}}{\kappa^2} & \frac{L_{01}}{\kappa^2} & \frac{-L_{01}R_{02}}{\kappa^2} & \frac{M_{01}R_{01}}{\kappa^2} \\ \frac{M_{01}}{\kappa^2} & \frac{-M_{01}}{\kappa^2} & \frac{M_{01}R_{02}}{\kappa^2} & \frac{-L_{02}R_{01}}{\kappa^2} \end{bmatrix} \quad B_1 = \begin{bmatrix} 0 \\ 0 \\ \frac{-M_{01}}{\kappa^2} \\ \frac{L_{02}}{\kappa^2} \end{bmatrix} \quad C_1 = [1 \quad 0 \quad 0 \quad 0] \quad D_1 = [0]$$

When Q_1 is in OFF mode, the state-space matrices are given by

$$\dot{x} = A_2 x + B_2 u \quad (18)$$

$$y = C_2 x + D_2 u \quad (19)$$

$$A_2 = \begin{bmatrix} \frac{-1}{R_{03}C_{02}} & 0 & \frac{1}{C_{02}} & 0 \\ 0 & 0 & 0 & \frac{-1}{C_{01}} \\ \frac{-L_{01}}{\kappa^2} & \frac{M_{01}}{\kappa^2} & \frac{-L_{01}R_{02}}{\kappa^2} & \frac{M_{01}R_{01}}{\kappa^2} \\ \frac{M_{01}}{\kappa^2} & \frac{-L_{02}}{\kappa^2} & \frac{M_{01}R_{02}}{\kappa^2} & \frac{-L_{02}R_{01}}{\kappa^2} \end{bmatrix} \quad B_2 = \begin{bmatrix} 0 \\ 0 \\ \frac{-M_{01}}{\kappa^2} \\ \frac{L_{02}}{\kappa^2} \end{bmatrix} \quad C_2 = [1 \quad 0 \quad 0 \quad 0] \quad D_2 = [0]$$

The duty cycle is expressed as D_u

$${D_u}^* \triangleq 1 - D_u \quad (20)$$

$$\frac{V_{OUT}}{V_{IN}} = \frac{D_u}{1-D_u} = \frac{D_u}{{D_u}^*} \quad (21)$$

The following outcomes are obtained for an SSA model of the Cuk converter.

$$A = A_1 D_u + A_2 {D_u}^* \quad (22)$$

$$B = B_1 D_u + B_2 {D_u}^* \quad (23)$$

$$C = C_1 D_u + C_2 {D_u}^* \quad (24)$$

$$D = D_1 D_u + D_2 {D_u}^* \quad (25)$$

$$X = -A^{-1} B V_{IN} \quad (26)$$

$$B_d = (A_1 - A_2)X + (B_1 - B_2)V_{IN} \quad (27)$$

$$D_d = (C_1 - C_2)X + (D_1 - D_2)V_{IN} \quad (28)$$

Here, A is the weighted average of A_1 for ON mode and A_2 for OFF mode. The same goes for B, C and D.

$$\bar{\dot{x}} = A\bar{x} + B\bar{v_{IN}} + B_d\bar{d} \quad (29)$$

$$\bar{v_0} = C\bar{x} + D\bar{v_{IN}} + D_d\bar{d} \quad (30)$$

A bar (-) displays a minor signal deviation from the nominal.

$$x = X + \bar{x} \quad (31)$$

$$v_{IN} = V_{IN} + \bar{v_{IN}} \quad (32)$$

$$d = D_u + \bar{d} \quad (33)$$

$$v_{OUT} = V_{OUT} + \bar{v_{OUT}} \quad (34)$$

$$A = \begin{bmatrix} \frac{-1}{R_{03}C_{02}} & 0 & \frac{1}{C_{02}} & 0 \\ 0 & 0 & \frac{-D_u}{C_{01}} & \frac{1-D_u}{C_{01}} \\ \frac{-L_{01}}{{L_{01}L_{02}-M_{01}}^2} & \frac{D_uL_{01}+M_{01}-D_uM_{01}}{{L_{01}L_{02}-M_{01}}^2} & 0 & 0 \\ \frac{M_{01}}{{L_{01}L_{02}-M_{01}}^2} & \frac{-D_uM_{01}-L_{02}-L_{02}D_u}{{L_{01}L_{02}-M_{01}}^2} & 0 & 0 \end{bmatrix} \quad B = \begin{bmatrix} 0 \\ 0 \\ \frac{-M_{01}}{{L_{01}L_{02}-M_{01}}^2} \\ \frac{L_{02}}{{L_{01}L_{02}-M_{01}}^2} \end{bmatrix} \quad C = [1 \quad 0 \quad 0 \quad 0] \quad D = [0]$$

$$B_d = \begin{bmatrix} 0 \\ \frac{-D_u V_{IN}}{R_{03}(1-D_u)^2 C_{01}} \\ \frac{V_{IN}(L_{01}-M_{01})}{(1-D_u)(L_{01}L_{02}-{M_{01}}^2)} \\ \frac{V_{IN}(L_{02}-M_{01})}{(1-D_u)(L_{01}L_{02}-{M_{01}}^2)} \end{bmatrix} \qquad D_d = [0]$$

The equilibrium state vector is

$$X = \begin{bmatrix} v_{02} \\ v_{01} \\ i_{02} \\ i_{01} \end{bmatrix} = \begin{bmatrix} \frac{D_u V_{IN}}{1-D_u} \\ \frac{V_{IN}}{1-D_u} \\ \frac{D_u V_{IN}}{R_{03}(1-D_u)} \\ \frac{{D_u}^2 V_{IN}}{R_{03}(1-D_u)^2} \end{bmatrix}$$

3. Open Loop Performance

Figure 2 shows a block diagram of the open-loop system. The disturbance-containing state space equations are

$$\dot{x} = Ax + BV_{IN} + B_d d \qquad (35)$$
$$V_{OUT} = Cx \qquad (36)$$
$$x = [v_{02} \quad v_{01} \quad i_{02} \quad i_{01}]' \qquad (37)$$

The SSA matrices (A, B, C, D) are the matrices from the disturbance input V_{IN} to V_{OUT} for the open loop model. For the controlled input d, the SSA matrices are (A, B_d, C, D). Thus, there are two inputs in this converter (disturbance input V_{IN} and a control input d) an output V_{OUT}. The circuit components of the Cuk converter are given in Table 2. With nominal D_u= 0.667, a 12V step input induces 24V output voltage. This shows that disturbance to the input voltage (V_{IN}) is not rejected by the open-loop system.

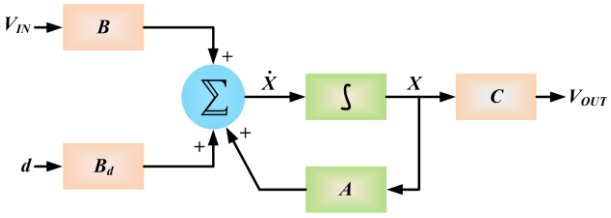

Figure 2. Cuk converter open loop model

4. Control Schemes

This section describes FSFB, FSFBI, ROSE, and LQR optimal control strategy, for the Cuk converter, in the following subsections.

4.1 FSFB controller

All the state variables are considered accessible for feedback and measurable in FSFB. The Cuk converter is a fully observable and controllable system. By using the state feedback matrix, the closed loop poles can be located via the feedback gain matrix at any desired position. The control law is

$$u = -kx \qquad (38)$$

where, k is the state feedback gain matrix. The closed loop poles can be located at any desired position by calculating the value of k in the complex plane. Ackerman's formula is used to find the value of k, and the proper choice of closed loop poles is done from Table 3.

After applying FSFB controller, the Cuk converter output does not follow the desired output voltage. The output voltage and stability based on the Bode plot are discussed in the results section.

Table 2. Circuit components of Cuk converter

Circuit components	Value
L_{01}	0.0005H
R_{01}	0.01Ω
L_{02}	0.0075H
R_{02}	0.01Ω
M_{01}	-0.0015mH
C_{01}	2×10^{-6}F
C_{02}	2×10^{-5}F
R_{03}	30Ω
V_{IN}	12V
D_u	0.667
f	1×10^{5}Hz

Table 3. Pole position after pole placement

Order	Pole placement
1	ω_1[-1]
2	ω_2[-0.7071±0.7071i]
3	ω_3[-0.521 ±1.068i; -0.708]
4	ω_4[-0.626 ± 0.4141i; -0.424 ± 1.263i]
5	ω_5[-0.5758±0.5339i; -0.8955; -0.3764 ± 1.292i]

4.2 FSFBI

After applying the FSFB controller, the Cuk converter has a maximum error of 0.24V after a unit step disturbance in the input voltage. To reduce this error, additional gain can be applied. The Cuk converter is a type zero system, which means that no matter how large the gain is in a regulated system, there is always some finite steady-state error from step disturbances. If the system type is increased, steady-state error can be eliminated. FSFB does not change the type as it has no integrator in the feedback. An integrator can be used to remove the steady-state offset. The integrator integrates error between output and the reference signal and then adds it to the state feedback control signal. After adding an integrator in the system, the Cuk converter becomes a fifth-order system. Now the state vector is $[v_{02} \quad v_{01} \quad i_{02} \quad i_{01} \quad x_i]'$ where x_i corresponds to reference error integral. The control law is

$$u = -kx - k_i x_i \qquad (39)$$

where k_i is state feedback integral gain matrix and k is controller gain. After adding the integrator to the system, the Cuk converter output reached 24.24V, and after 2ms, it is

maintaining 24V, but more improvement is needed. The output voltage and stability based on the Bode plot are discussed in the results section.

4.3 ROSE

During FSFB controller, all states were considered measurable and available for feedback, but this does not happen in reality. ROSE estimates the unmeasured states of the Cuk converter model, and the unmeasured states are v_{01}, i_{02} and i_{01} while v_{02} is a measured state. Thus, it is necessary to estimate only three unmeasured states. The linear control law is

$$u = -k_m x_m - k_u x_u \tag{40}$$

where, k_m is measured state feedback gain matrix, k_u is the unmeasured state feedback gain matrix, x_m denotes the states that exist in the measurement equation's output, and x_u denotes the remaining unmeasured states. The poles of reduced order are located so as to achieve faster dynamics than controlled system poles. The output voltage and stability based on the Bode plot are discussed in the results section.

4.4 LQR control

LQR applies penalties on control effort (u) and state transient (x) w.r.t. a figure of merit calculated as a cost function, to maximize system performance. The best way to control state changes and regulate effort within output specifications is to use a compensator that tries to have a control strategy which minimises a Lagrangian cost function.

$$J = \int_0^\infty (x^T Q x + u^T R u) dt \tag{41}$$

subject to state equation constraints

$$\dot{x} = Ax + Bu \tag{42}$$

This is called the LQR problem. The weight matrix Q is a positive semi-definite $(n \times n)$ matrix that penalizes variation of the state from the desired state (for a system with *n* states). A positive definite matrix $(m \times m)$ that penalizes control effort is the weight matrix *R*. The time-invariant solution to this problem is

$$K = R^{-1} B^T P \tag{43}$$

where *P* is a symmetric, positive definite solution to the Riccati equation in a steady state.

$$PA + A^T P - PBR^{-1}B^T P + Q = 0 \tag{44}$$

As both the weight matrices R and Q are carried within the cost function and summed, it is imperative that the weights for each quadratic form are in reasonable proportions. As the Cuk converter is a fifth order system, Q is a (5×5) matrix. Therefore, for the LQR to develop a positively definite semi-defined Q-Matrix there are two positive entries corresponding to the first (Q_{11}) and last (Q_{55}) diagonal entries. The Cuk converter is designed to have one control input and was randomly set to 1 for initial design R. The chosen Q and R matrices are given below

$$Q(1,1) = 1;\ Q(2,2) = 0;\ Q(3,3) = 0;\ Q(4,4) = 0;\ Q(5,5) = 100000;\ R = 1;$$

After applying LQR, the Cuk converter output reached its maximum of 24.02V and, after 14 ms, maintained the desired 24V output, during unit step disturbance. The output voltage and stability based on the Bode plot are discussed in the results section.

5. Results and Discussion

MATLAB was used to build the Cuk converter model. The Cuk converter's dynamic output is reviewed for the open loop system and for the various control schemes discussed in previous sections. A comparative review of all the findings is also carried out in this section.

5.1 Open loop performance

The output of the open-loop Cuk model was tested before designing a controller. Figure 3 illustrates an open-loop response in V_{IN} to a unit step disturbance. It is found out that system generated lightly damped oscillations around the steady state in the plotted response. Using equation (2), the expected value is 26V at a steady state. There is fluctuation in the output, which is undesirable. With nominal D_u = 0.667, a 12V step input induces 24V output voltage. This shows that disturbance to the input voltage (V_{IN}) is not rejected by the open-loop system. Since the duty cycle must lie between 0 and 1, if control effort or nominal value exceeds the limiting value, i.e., 0.667, the design of the compensator is not acceptable. A gain margin of at least 20 dB and a phase margin of at least 50 degrees is needed to guarantee stability.

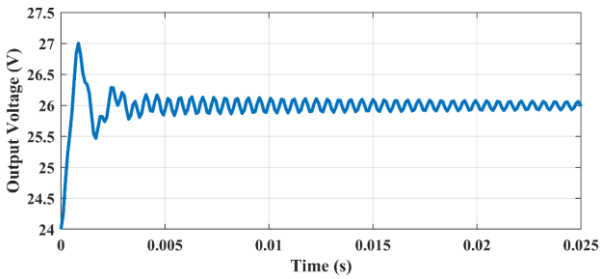

Figure 3. Open-loop response of input voltage to a unit step disturbance

5.2 FSFB controller

The main objective is for the Cuk converter output to obey a constant value for instance, V_{OUT} = 24V (when V_{IN} = 12V and D_u = 0.667), despite potential disturbances, which is not obtained with the open loop system. The Cuk converter output voltage with FSFB controller under unit step disturbance is displayed in Figure 4. The maximum output voltage is 24.24V. So, the maximum error here is 0.24V, and it must be further reduced. The stability of the system is determined using a Bode plot. The gain and phase margins obtained by MATLAB

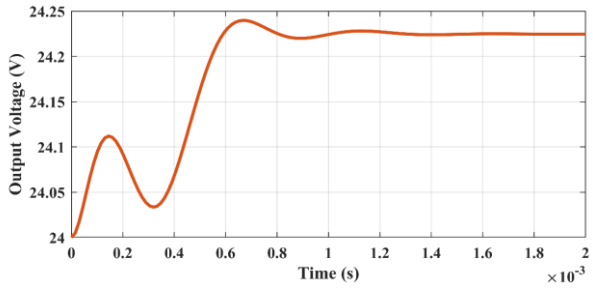

Figure 4. FSFB controller response to a unit step disturbance of input voltage

calculations are infinite and 66.7 degrees, respectively, which are highly appealing features for frequency domain response. So, the system is stable.

5.3 FSFBI controller

The output voltage response to unit step disturbance of Cuk converter with FSFBI control is displayed in Figure 5. The maximum output voltage was 24.24 V, but after 2 ms the output voltage was near 24 V. The stability of the system was assessed from a Bode plot. The gain margin was infinite and the phase margin was 77.5 degrees, calculated using MATLAB. These follow the requirements of the design. Hence, stability of the system is secured. Note that -0.018 is the final value of the control signal. This is the estimated modification in the duty cycle needed to eliminate V_{IN} unit step disturbance.

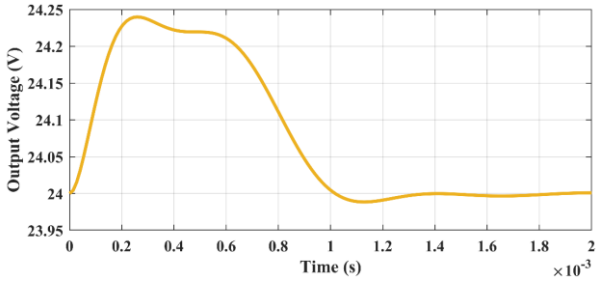

Figure 5. Response to unit step disturbance with FSFBI controller

5.4 ROSE

The response to unit step disturbance with ROSE control is shown in Figure 6. The maximum output voltage was 24.12 V, but after 1.7 ms, the output voltage was near 24 V. The gain margin was -24.9 dB and the phase margin 36.4 degrees. These do not follow the design requirements, and uncertainty can make the managed system unstable. So, it is necessary to apply another method to stabilize the system.

5.5 LQR

The response to unit step disturbance of Cuk converter output voltage with LQR control is illustrated in Figure 7. The maximum output voltage was 24.02 V, i.e., very accurate, and within a second the output voltage was 24 V. The duration of transient from unit step disturbance with the LQR

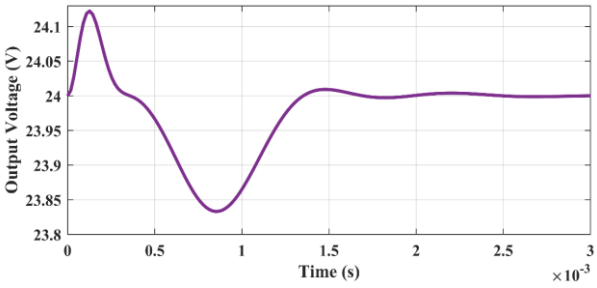

Figure 6. Response to unit step disturbance with ROSE control

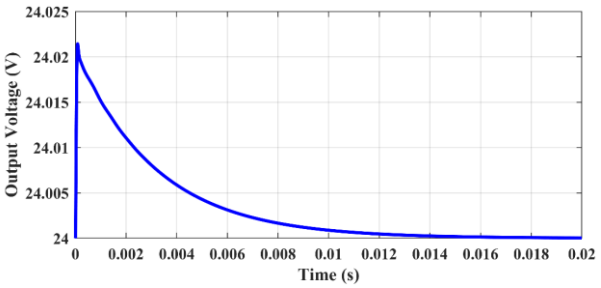

Figure 7. Response to a unit step disturbance in input voltage with LQR control

compensator was found to be substantially longer than the settling times with the previously tested controllers. The amplitude deviation, however, was substantially lower. As the performance requirements are still fulfilled, this is a reasonable design trade-off. The Bode plot of the Cuk converter with LQR under unit step disturbance is shown in Figure 8. It can be seen that the LQR built for a SISO system possesses very desirable stability properties. It will always have a phase margin of at least 60 degrees and a gain margin between -6 dB and infinity.

Figure 9 shows a comparative analysis of the four control schemes during disturbance. It is evident that LQR control instantly tracks the desired response with negligible fluctuation, while the other approaches have a significant amount of deviations from target.

Table 4 shows details of performance analysis with the various control schemes, in terms of gain margin, phase margin, duration of transients, and initial output voltage. It is seen that the Cuk converter in an open loop has continuous fluctuations, FSFB controller maintained a persistent error of 0.24 V, FSFBI eliminated the error but the response was fluctuating, ROSE had both overshoot and undershoot being undesirable, while the proposed LQR scheme smoothly achieved the desired output voltage and had gain and phase margins within the limits guaranteeing system stability.

Finally, the robustness of the proposed LQR control of Cuk converter against disturbances is compared to state-of-the-art methods. These techniques involve averaged Cuk model (Selwan, Park, & Gajic, 2015), Loop shaping method (Rayeen, Bose, & Dwivedi, 2018), PID-GA (Poudeh, Eshtehardiha, & Ershadi, 2008), and Pole placement-PSO (Yousefi, Emami, Eshtehardiha, & Poudeh, 2008).

Figure 10 depicts the Cuk converter response along with other control schemes. It is seen that the LQR approach takes only 14 ms to settle down during unexpected disturbances, whereas the averaged Cuk model, Loop shaping

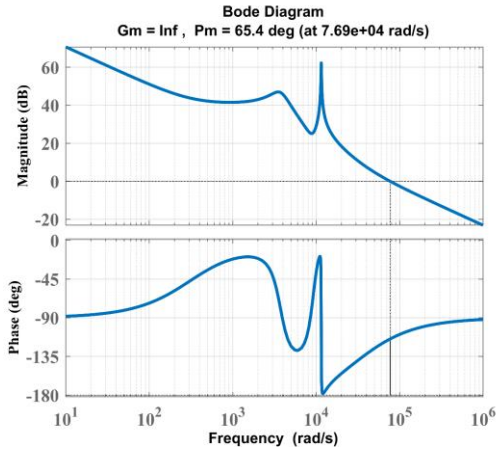

Figure 8. LQR compensator loop gain of Cuk converter

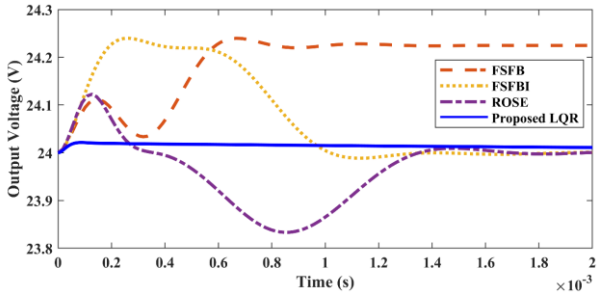

Figure 9. Comparative analysis of control schemes during disturbance

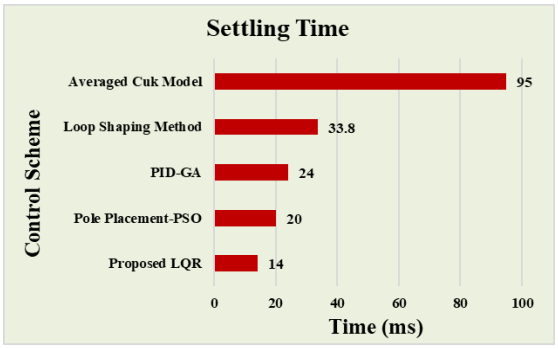

Figure 10. Cuk converter response with alternative control schemes

6. Conclusions

This article presented the control and modeling of Cuk converter with various control schemes tested against unit step disturbance in CCM. The SSA technique defines the linear Cuk converter model and gives a fourth-order transfer function. A comparative analysis of control schemes was done for FSFB controller, FSFBI, ROSE and the proposed LQR, using MATLAB. The steady-state error cannot be entirely removed because the Cuk converter is a type zero system. So, an integrator is employed to increase the type of the system. The MATLAB results showed that LQR was the most effective among the tested control techniques, minimizing the steady-state error. In addition, the system's stability was not affected by a unit step disturbance. Finally, the robustness of the proposed LQR was also compared to state-of-the-art control schemes, namely averaged Cuk model, loop shaping method, PID-GA, and pole placement-PSO. The findings demonstrate the superiority of the suggested LQR approach. Therefore, the LQR approach is the recommended choice for control of a Cuk converter, optimizing the Cuk converter performance specifications.

References

Aboulnaga, A. A., & Emadi, A. (2004). High performance bidirectional Cuk converter for telecommunication system. *Proceeding of the 26th Annual International Telecommunication Energy Conference*, 182–189.

Amini, A., & Nazarzadeh, J. (2008). Improvement behavior and chaos control of Ćuk converter in current mode controlled. *IEEE International Conference on Industrial Technology*, 1-6.

Balestrino, A., Landi, A., & Sani, L. (2002). Cuk converter global control via fuzzy logic and scaling factors. *IEEE Transactions on Industry Applications*, *38*(2), 406–413.

Chong, BVP., & Zhang, L. (2013). Controller design for integrated PV-converter modules under partial shading conditions. *Solar Energy*, *92*, 123 - 138.

Chung, H. S. H., Tse, K. K., Hui, S. Y. R., Mok, C. M., & Ho, M. T. (2003). A novel maximum power point tracking technique for solar panels using a SEPIC or Cuk converter. *IEEE Transactions on Power Electronics*, *18*(3), 717–724.

Chen, Z. (2012). PI and sliding mode control of a Cuk converter. *IEEE Transactions on Power Electronics, 27*(8), 3695–3703.

Cuk, S., & Middlebrook, R.D. (1983). Advances in switched-mode power conversion Part I. *IEEE Transactions on Industrial Electronics*, *30*(1), 10–19D

Cuk, S., & Middlebrook, R.D. (1983). Advances in switched-mode power conversion Part II. *IEEE Transactions on Industrial Electronics*, *30*(1), 19–29.

De Britto, J. R., Demian, A. E., De Freitas, L. C., Farias, V. J., Coelho, E. A. A., & Vieira, J. B. (2008). A proposal

Table 4. Details of performance measures with the various control schemes

Control Scheme	Initial output voltage	Time to reach desired output voltage	Gain margin	Phase margin
Open loop	26V	Continuous fluctuation	-	-
FSFB	24.24V	Persistent error	Infinite	66.7 deg.
FSFBI	24.24V	2ms (fluctuating)	Infinite	77.5 deg.
ROSE	24.13V	1.7ms (fluctuating)	-24.9 dB	36.4 deg.
Proposed LQR	24.02V	14ms (Smooth)	Between (-6 dB, infinite)	60 deg.

of led lamp driver for universal input using Cuk converter. *IEEE Power Electronics Specialists Conference*, 2640–2644.

Fan,Y., Ge, L. M., & Hua, W. (2010). Multiple-input DC–DC converter for the thermoelectric-photovoltaic energy system in hybrid electric vehicles. *IEEE Vehicle Power Propulsion Conference*, 35–40.

Flores, J. L., Avalos, J. L. B., & Espinoza, C. A. B. (2011). Passivity-based controller and online algebraic estimation of the load parameter of the DC-to-DC power converter Cuk type. *IEEE Latin America Transactions, 9*(1), 50–57.

Himmelstoss, F., & Walter, C.M. (2010). A simple cuk converter derivated two-quadrant DC motor controller. *Proceeding of the International Symposium on Power Electronics, Electrical Drives, Automation and Motion*, 1108-1112.

Janjornmanit, S., Yachiangkam, S., & Kaewsingha, A. (2007). Energy harvesting from exercise bicycle. *Proceeding of the 7th International Conference Power Electronics Drive System*, 1138–1140.

Jose, P., & Mohan, N. (2003). A novel ZVS bidirectional Cuk converter for dual voltage systems in automobiles. *Proceeding of the 29th Annual Conference IEEE Industrial Electronics Society, 1*, 117–122.

Kathi, L., Ayachit, A., Saini, D.K., Chadha, A., & Kazimierczuk, M. K. (2018). Open-loop small-signal modeling of Cuk DC-DC converter in CCM by circuit-averaging technique. *IEEE Texas Power and Energy Conference*, 1–6.

Kugi, A., & Schlacher, K. (1999). Nonlinear H-infinity controller design for a DC-to-DC power converter. *IEEE Transactions on Control System Technology, 7*(2), 230–237.

Lekić, A., Stipanović, D., & Petrović, N. (2018). Controlling the Ćuk Converter Using Polytopic Lyapunov Functions. *IEEE Transactions on Circuits and Systems II, 65*(11), 1678-1682.

Manna, S., Singh, D. K., & Akella, A. K. (2023). A Review of Control Techniques for Wind Energy Conversion System. *International Journal of Engineering and Technology, 13*(1), 40-69.

Mahdavi, J., Nasiri, M. R., Agah, A., & Emadi, A. (2005). Application of neural networks and state-space averaging to DC/DCPWM converters in slidingmode operation. *IEEE/ASME Transactions on Mecha tronics, 10*(1), 60–67.

Mcgee, B. R., & Nelms, R. M. (2004). Powering solid state radar T/R module arrays from a fuel cell using an isolated Cuk converter. *Proceeding of the 19th Annual IEEE Applied Power Electronics Conference Exposition, 3*, 1853–1857.

Medagam, P., & Pourboghrat, F. (2006). Nonlinear robust control of Cuk converter using radial basis functions. *Proceeding of the 38th North American Power Symposium*, 229–234.

Neely, J., Decarlo, R., & Pekarek, S. (2010). Real-time model predictive control of the C´uk converter. *IEEE 12th workshop Control Modeling Power Electronics*, 1–8.

Pietkiewicz, A., & Tollik, D. (1988). Modeling and analysis of the current mode controlled Cuk converter with coupled inductors. *IEEE Power Electronics Specialists Conference, 1*, 398-405.

Poudeh, M. B., Eshtehardiha, S., & Ershadi, M. H. (2008). Optimizing the classic controllers to improve the Cuk converter performance based on genetic algorithm. *Proceeding of International Conference on Smart Manufacturing Application*, 329– 334.

Rayeen, Z., Bose, S., & Dwivedi, P. (2018, December). Study of closed loop Cuk converter controlled by loop shaping method. *Proceeding of 2018 IEEE 13th International Conference on Industrial and Information Systems* (*ICIIS*) (pp. 442-447).

Safari, A., & Mekhilef, S. (2011). Simulation and hardware implementation of incremental conductance MPPT with direct control method using Cuk converter. *IEEE Transactions on Industrial Electronics, 58*(4), 1154–1161.

Selwan, E., Park, G., & Gajic, Z. (2015). Optimal control of the Cuk converter used in solar cells via a jump parameter technique. *IET Control Theory and Applications, 9*(6), 893-899.

Singh, S., & Singh, B. (2010). A voltage-controlled PFC Cuk converter based PMBLDCM drive for air-conditioners. *IEEE Industry Applications Society Annual Meeting*, 1–6.

Sira-Ramírez, H., & Silva-Ortigoza, R. (2006). *Control design techniques in power electronics devices*. Mexico**:** Springer Science and Business Media.

Su, G., Gong, W., Pan, L., Gao, R., & Wang, B. B. (2010). Maximum power point tracing of photovoltaic cells with OIF-Elman network. *Proceeding of the 29th Chinese Control Conference*, 4880–4884.

Thangavelusamy, D., & Thirumeni, M. (2019). Design and analysis of hybrid PSO–GSA tuned PI and SMC controller for DC–DC Cuk converter. *IET Circuits, Devices and Systems, 13*, 374-384.

Tse, C. K., Lai, Y. M., & Iu, H. H. C. (2000). Hopf bifurcation and chaos in a free-running current-controlled Cuk switching regulator. *IEEE Transactions on Circuits System, 47*(4), 448–457.

Umamaheswari, M., & Uma, G. (2013). Analysis and design of reduced order linear quadratic regulator control for three phase power factor correction using Cuk rectifiers. Electric Power System Research, 96, 1–8.

Wong, S. C., Wu, X. Q., & Tse, C. K. (2008). Sustained slow-scale oscillation in higher order current-mode controlled converter. IEEE Transactions on Circuits System, 55(5), 489–493.

Xu, D., Zhao, C., & Fan, H. (2004). A PWM plus phase-shift control bidirectional dc-dc converter. IEEE Transactions on Power Electronics, 19(3), 666–675.

Yousefi, M. R., Emami, S. A., Eshtehardiha, S., & Poudeh, M. B. (2008, December). Particle swarm optimization and genetic algorithm to optimizing the pole placement controller on Cuk converter. In 2008 IEEE 2nd International Power and Energy Conference (pp. 1461-1465). IEEE.

Zane, R., & Maksimovic, D. (1998). Nonlinear-carrier control for high-powerfactor rectifiers based on up–down switching converters. IEEE Transactions on Power Electronics, 13(2), 213–221.